Electron distribution and level occupation in an ensemble of $In_xGa_{1-x}As/GaAs$ self-assembled quantum dots

W.-H. Chang and T. M. Hsu
Department of Physics, National Central University, Chung-Li, Taiwan 32054, Republic of China

N. T. Yeh and J.-I. Chyi
Department of Electrical Engineering, National Central University, Chung-Li, Taiwan 32054, Republic of China

(Received 8 November 1999; revised manuscript received 21 August 2000)

We presented capacitance-voltage characteristics and electron-filling reflectance measurements to investigate electron distribution in $In_{0.5}Ga_{0.5}As$ self-assembled quantum dot ensemble. First, the electronic structures of the quantum dots were constructed by capacitance-voltage profile. Coulomb charging effects on the electronic structures were also discussed. Then, the electron level occupations were investigated by the electron-filling reflectance spectra. Due to the correlated carrier transfer among the quantum dots and the *n*-type GaAs environment, the electron level filling is found to be inhomogeneous near the Fermi level. Finally, electron thermal population in the quantum dot levels was also investigated. The activation energies for the thermal population were found to be close to the level splitting. This means that electrons thermally populated to higher state do not require Coulomb charging energy.

I. INTRODUCTION

The zero-dimensional quantum dot (QD) systems have recently been of considerable interest in the field of semiconductor physics.[1,2] Driven by the progressing in material growth techniques, fabricating a self-assembled QD system can now be easily achieved by using a lattice-mismatch semiconductor system in the Stranski-Krastanow (SK) growth mode. The fascinating properties exhibited by QD's have also been proposed as useful applications in optoelectronic devices,[3–7] such as QD lasers[3,4] and optical memory devices.[5–7] For these device applications to be realistic, the electrical and optical properties of QD's, such as the interband and intersubband carrier dynamics,[8,9] the Coulomb interactions[10–15] and the carrier distributions,[16–18] has been widely investigated. Of these studies perhaps the greatest lack is the carrier distributions in the QD ensemble, which however, may be a basic issue for these device applications.

Several studies[16–18] have addressed the issue of carrier distributions in the QD's using low-temperature photoluminescence (PL) experiments. Dynamical carrier distributions are deduced from the competition between several dynamic processes, including the carrier generation, capture, thermionic emission, recombination rates, and even the intersubband relaxation rates. In this study, we intended to investigate a static (or quasistatic) carrier distribution in the QD ensemble. Of the many experimental techniques for investigating the carrier distribution, the most often used is the capacitance-voltage (C-V) characteristics.[19–22] For a QD layer embedded in space-charge structures, which are commonly used in deep-level transient spectroscopy (DLTS),[23] the C-V measurement has been proven to be a powerful tool for characterizing the charge accumulation in the QD layer. However, to obtain the QD's electronic confinement energies and level occupations, one has to process sophisticated self-consistence calculations to fit the experimental results.[21]

More recently, it has been proposed that electron level occupations in the QD's can also be obtained from the electron-filling reflectance (EFR) spectra.[22] Due to the Pauli-blocking effect, the EFR spectra reveal the quasistatic electron level occupations in the QD's. In this paper, we shall demonstrate results both from the C-V and the EFR experiments. Firstly, the electronic structures of the QD's were constructed by the C-V measurements. The possible contributions of Coulomb charging effect are also discussed. Then the electron level occupations were investigated using the EFR measurements. The electron distribution in the QD ensemble, which considers *inhomogeneity* among the dots, is also presented. Finally, the temperature effects on the electron thermal population in the QD's were demonstrated.

II. EXPERIMENTS

The investigated samples were fabricated by molecular beam epitaxy in the SK growth mode on a n^+-doped (001) GaAs substrate. After the deposition of a 300 nm n^+-doped GaAs buffer layer and an 100 nm n-doped [Si, $N_d \sim (7\pm1)\times10^{16}\,\mathrm{cm}^{-3}$] GaAs layer, a self-assembled $In_{0.5}Ga_{0.5}As$ QD's layer ($\approx$5 ML) was deposited. The onset of spontaneous islanding occurred at about 2.3–2.5 ML $In_{0.5}Ga_{0.5}As$ deposition, which has been confirmed by the reflection high-energy electron diffraction (RHEED) pattern. After the formation of QD's the layer structure was capped with a 300 nm n-doped [Si, $N_d \approx (7\pm1)\times10^{16}\,\mathrm{cm}^{-3}$] GaAs layer and completed by capping a p^+-doped GaAs layer to form a p^+-n junction. In this work, two samples were investigated. Samples A and B contain the same layer structure, but having slightly different dot size and density. According to the transmission electron microscopy (TEM) images, both samples show that the QD's were lens shaped, being 3.5 $\pm$0.5 nm high in the growth direction. In sample A, the average QD diameter is smaller, which is found to be $\sim$15 nm and a dot density of $n_{\mathrm{dot}} \approx 1\times10^{11}\,\mathrm{cm}^{-2}$. The QD's in sample B have a larger average diameter of $\sim$23 nm, with a

0163-1829/2000/62(19)/13040(8)/$15.00 PRB 62 13 040 ©2000 The American Physical Society

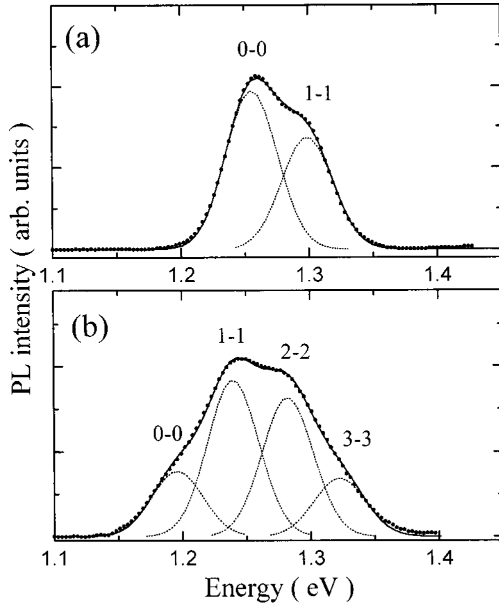

FIG. 1. The PL spectra measured at $T=10\,\mathrm{K}$ for sample A (a) and sample B (b).

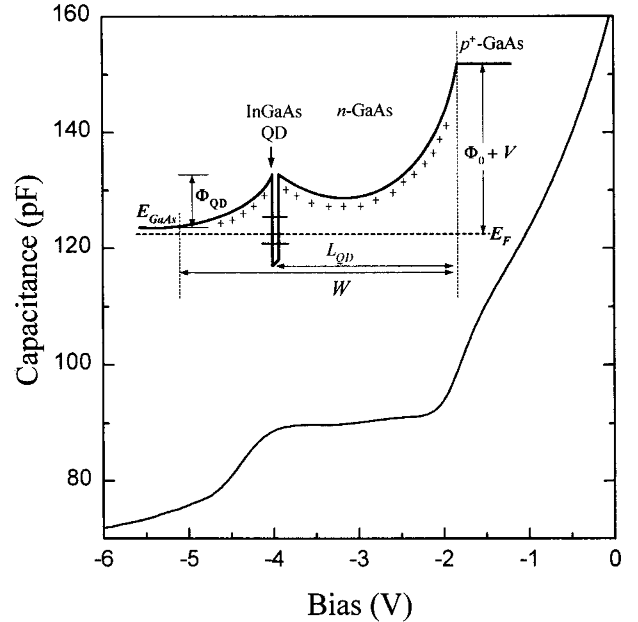

FIG. 2. The C-V profile measured at $T=10\,\mathrm{K}$ for sample A. The inset shows the conduction-band profile for the investigated sample under reversed bias.

lower density of $n_{\mathrm{dot}}\approx 4\times 10^{10}\,\mathrm{cm}^{-2}$.

The C-V characteristics were measured by a HP 4284A (20 Hz-1 MHz) LCR meter with a 5 mV test signal. Before performing the C-V measurements, 500 μm mesa squares were etched to a depth of $\sim$1 μm and a Au/Be film with 250 μm square apertures was deposited on the sample surface to form ohmic front contacts. The experimental arrangement for the EFR was the same as that for the conventional electroreflectance. First, a light from an 1 kW tungsten-halogen lamp combined with a 0.5 m monochromator was focused onto the sample. Then an ac (square-wave) modulation voltage ($\sim$200 Hz) composed of a dc bias was applied to the sample. Finally, the modulated reflectance ΔR was detected by a LN_2 cooled Ge detector, with the standard lock-in techniques.

III. RESULTS AND DISCUSSION

A. Electronic structures and charge accumulation

The investigated samples were first characterized by the PL measurements. Figures 1(a) and 1(b) displayed the PL spectra for samples A and B measured at $T=10\,\mathrm{K}$. These spectra were excited by the 514.5 nm line of an Ar^+ laser with an excitation power of about $\sim$1 $\mathrm{kW/cm^{-2}}$. In Fig. 1, each spectrum shows multiple peaks, which were confirmed to be the ground state and excited states luminescence by the use of state-filling spectroscopy.[8,24] As deduced from a multiple Gaussian fit, these spectra show an interlevel spacing of $\Delta E_{01}=45\pm 5$ meV, and a linewidth of $\Gamma\approx 40\,\mathrm{meV}$. We also noted that the QD ground-state energy for sample A ($E_0=1.255\,\mathrm{eV}$) is about 60 meV higher than that for the sample B ($E_0=1.196\,\mathrm{eV}$), which may be due to the slightly smaller QD size and higher QD density in sample A.[25]

Figure 2 shows the C-V profile for sample A measured at $T=10\,\mathrm{K}$. In the bias range of $-4.4\ \mathrm{V}<V_b<-2\ \mathrm{V}$, a pronounced capacitance plateau[21] due to the carrier accumulation in the QD layer was observed. For the doping concentration in n-type GaAs and the QD layer location in this sample, the QD layer was expected to be loaded with some electrons at zero bias. As a reversed bias was applied, electrons in the QD layer will be removed, forming a capacitance plateau ($V_b<-2$ V) when the depletion region of the p^+-n junction meets the QD layer (see the inset of Fig. 2). Further decreasing the V_b, the Fermi level E_F would be gradually moved down through the electronic states of the QD's. As were shown in more detail in Fig. 3(a), sample A resolved two steps in the capacitance plateau. They were assigned to the charging of the QD ground state and the first excited state, which have been confirmed by the EFR measurements discussed below. For the case of sample B in Fig. 3(b), we resolved three steps in the capacitance plateau. According to the TEM images, the QD density of sample B is about 2–3 times smaller than that of sample A. Thus, it is very reasonable that the electrons were filled up to the third QD excited states in sample B.

Because the E_F crossing the QD plane is not varied linearly with the applied bias in this space-charge structure, a sophisticated calculation seems to be unavoidable to deduce QD's parameters from these C-V profiles. It has been proposed that a quasistatic model involving some self-consistence calculations of Poisson equation will determine these confinement energies.[21] However, some depletion approximations are still possible, which is also an intention of this work. For example, when the depletion width of the p^+-n junction extends to the QD layer, the two-dimensional electron density in the QD layer, the depletion width w, and the applied bias V_b can be related by

$$\Phi_0-V_b=\frac{N_d}{2\varepsilon\varepsilon_0}w^2-\frac{Nn_{\mathrm{dot}}}{\varepsilon\varepsilon_0}L_{\mathrm{QD}},\qquad(1)$$

where Φ_0 is the built-in potential, N is the mean-electron occupation in the QD's, and L_{QD} is the nominal distance of

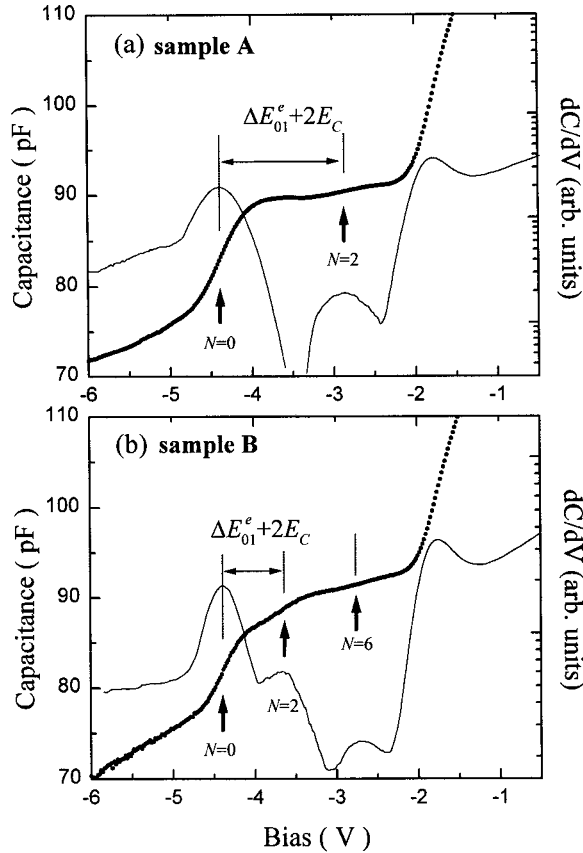

FIG. 3. The capacitance plateaus of electrons charging to the QD state appeared in *C-V* characteristics for sample A (a) and sample B (b). The corresponding derivative curves (dC/dV) are also included.

the QD layer (300 nm) below the p^+-n interface. The first term appeared in the right-hand-side of Eq. (1) represents the electrostatic potential at the p^+-n interface caused by the positive ionized donor in the depletion region, and the second term is contributed by the effect of carrier accumulation in the QD layer. Once the mean QD occupation N is known at a given V_b, the depletion width w can be determined. Accordingly, the E_F across the QD layer can be estimated by the potential bending of the GaAs conduction band below the QD layer,

$$\Phi_{\rm QD}=qN_d(w-L_{\rm QD})^2/2\varepsilon\varepsilon_0. \tag{2}$$

In Fig. 3(a), the first capacitance step represents the charging of the twofold degenerate QD ground state, i.e., the *s*-shell. For bias below -4.4 V the QD's are empty, and the *C-V* profile shows a characteristic of a pure junction capacitance. At $V_b=-4.4$ V electrons start to be charged into the QD ground state. At this bias, the E_F should be just below the threshold energy for charging the first electron into the *s*-shell. By the use of Eqs. (1) and (2) with $N=0$ at $V_b=-4.4$ V we deduced a band bending of $\Phi_{\rm QD}=166$ meV. This suggests that the QD ground-state energy may be roughly $E^e_0\approx-166(\pm10)$ meV, if we take an energy reference of $E=0$ eV at the GaAs conduction band edge. Despite this simple approximation, the estimated E^e_0 is very reasonable, as can be compared with the PL spectra. In Fig. 1(a), the PL spectrum shows a ground-state transition energy of $E_0=1.255$ eV, which gives an interband band discontinuity of $\approx$265 meV with respect to the GaAs band gap ($E_{\rm GaAs}=1.52$ eV). The value of $\approx$166 meV is quite close to a ratio of 2:1, for the energy splitting of electron and hole levels, which has been reported previously in InAs dots.[26]

At $V_b=-3.0$ V the electrons were starting to be charged into the first excited state (*p*-shell) of the QD's. Also from Eqs. (1) and (2), with $N=2$ at $V_b=-3.0$ V, we obtained an energy of $E^e_1\approx-88(\pm10)$ meV for the first QD excited state. This energy can be interpreted as the onset for charging the third electron into the QD *p*-shell. Interestingly, the energy difference for these two electron levels ($\approx$78 meV) is quite large, as compared with the interband energy splitting of $\Delta E_{01}=45$ meV in the PL spectra. We believe that the Coulomb charging effect plays a crucial role to the QD features appeared in *C-V* characteristics. For a small disk-shaped QD with a diameter d, the Coulomb charging energy required to charge an additional electron into the QD is given by $E_C=e^2/C$, where $C=4\varepsilon\varepsilon_0 d$ is the self-capacitance of the QD. For a typical InGaAs QD diameter of $d\approx15$ nm observed in sample A, we estimate a charging energy of $E_C\approx23$ meV. Taking the Coulomb charging effect into account, it requires an additional charging energy of $2E_C$ to put the third electron into the *p*-shell, with respect to the charging of the first electron into the *s*-shell. From this argument, the electron level splitting may be roughly $\Delta E^e_{01}=78$ meV $-2E_C\approx32$ meV. This value can be compared with the PL spectra. If we assume a ratio of 2:1 for the electron/hole level splitting,[26] the value of $\Delta E_{01}=45$ meV indicates an electron level splitting of $\Delta E^e_{01}\approx30$ meV which is very close to the value of $\approx$32 meV determined from our *C-V* measurements.

For the case of sample B, the same argument was applied. Also from the band bending deduced by Eqs. (1) and (2), the confined energies for the ground, first and second excited states of the QD's were found to be $E^e_0\approx-216$ (±10) meV, $E^e_1\approx-157(\pm10)$ meV, and $E^e_2\approx-81$ (±10) meV, respectively. These energies correspond to the onset for charging the first, third, and seventh electron into the QD states. For a typical QD diameter of $d\approx23$ nm found in sample B, we estimate a Coulomb charging energy of $E_C\approx15$ meV. Thus the electron level splitting for sample B is roughly $\Delta E^e_{01}=59$ meV $-2E_C\approx29$ meV, which is still in good agreement with the PL spectra.

B. Electron level occupations

Figure 4 shows one typical EFR spectrum for sample A measured at $T=10$ K, with a bias modulation between 0 V and -5.5 V. In this spectrum, two QD transitions are observed, ($E_0=1.25$ eV and $E_1=1.295$ eV), which are very close to the PL peaks observed in Fig. 1(a). The spectral feature near 1.37 eV is the WL signal. The schematic diagram in the inset of Fig. 4 can explain the mechanism for the EFR signals. According to the *C-V* profile in Fig. 3(a), the QD's are empty at -5.5 V, all the QD transitions are allowed. Consider that the QD's are partially filled at 0 V, say $N=3$ (two electrons in the ground state and one in the excited state), the interband transitions of these occupied states will be blocked. The EFR signals represent a reflectance change between these two charging states. Thus, the EFR

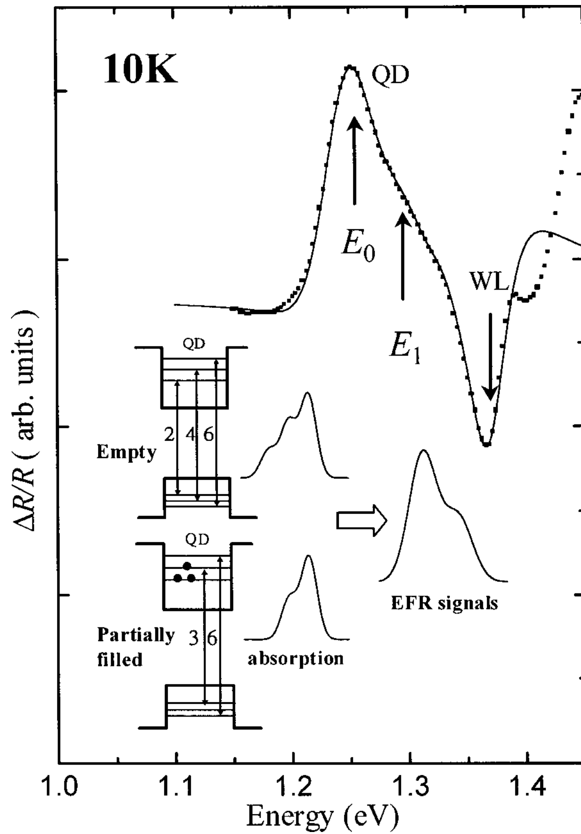

FIG. 4. The 10 K EFR spectrum (symbols) and the lineshape fitting curve (solid line). The inset shows a schematic diagram of the EFR modulating mechanism.

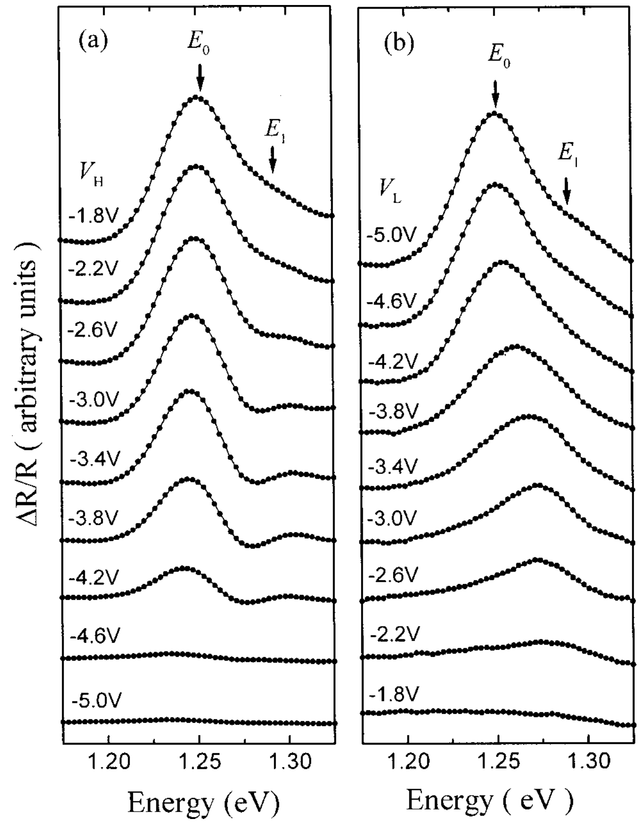

FIG. 5. Bias dependent EFR spectra for sample A in filling mode (a) with $V_L = -5.5$ V and in depletion mode (b) with $V_H = 0$ V.

intensities can be correlated to the electron level occupancy of the QD's. In Fig. 4, only two transitions were observed, indicating that at most two QD electron states are filled, which can be compared with the two-step features appeared in the *C-V* profile.

Based on this electron-filling feature discussed above, performing a bias dependent EFR measurement can give more information on the electron level filling in QD's. During the EFR measurements, the applied bias was modulated between two bias voltages, V_L and V_H. The higher bias, V_H, was selected for filling the electrons into the QD states, while the lower bias, V_L, was chosen for depleting the electrons from the QD's. In fact, the applied bias is very similar to the filling pulse and the detection bias, which were commonly used during the DLTS measurement. The main discrepancy is that the DLTS measured the change in capacitance transient ($\Delta C/C$), while the EFR measured the reflectance change ($\Delta R/R$) due to the electron moving in and out of the QD's. In this work, two kinds of bias-dependent EFR were carried out, one is the *filling* mode and the other is the *depletion* mode. The *filling* mode is that fixing the V_L at a larger reversed bias to deplete all the QD electrons, and varying the V_H for filling the electrons into the QD states. Alternatively, the *depletion* mode has a fixed V_H but varying the V_L.

Figure 5(a) shows the EFR spectra for sample A under filling mode, with a fixed $V_L = -5.5$ V and varied V_H. With the increasing V_H, the E_0 transition was first increased at lower V_H, then gradually saturated, accomplishing by the appearance of the E_1 transitions. It means that the electrons are first filled to the ground state, then filled to the first excited state at higher bias. In Fig. 5(b), we also show the EFR spectra in depletion mode, with a fixed $V_H = 0$ V and various V_L. As the V_L was decreased, the electrons at first excited state were first depleted, and then the ground-state electrons were fully evacuated at larger reversed bias. To analyze these EFR intensities, we use an intensity-modulated lineshape model, which is discussed in appendix. The bias-dependent EFR intensities were depicted in Fig. 6. Interestingly, we find an excellent correlation of these bias dependent intensities with the charging steps appeared in the *C-V* profile. In Fig. 6(a), the E_0 transition starts to increase at $V_H > -4.4$ V which is just the onset of the first charging step in Fig. 3(a). For $V_H > -3.0$, the E_1 transition appeared, which is also consistent with the second step which appeared in the *C-V* profile. Thus the assignment of these charging steps is clarified without ambiguity. Moreover, the saturated intensity of the E_1 transition suggests that the first excited state may be partially filled. Since the QD ground state is expected to be twofold degenerate, from the ratio of the E_0 and E_1 intensity, we estimate an average occupancy of ≈2–3 electrons per dot in sample A, at zero bias.

For the case of sample B, the EFR spectra with various filling biases (V_H) were displayed in Fig. 7. Here, we also include a PL spectrum for comparison. In these spectra, the state-filling feature can be seen more clearly, and the transition energies are close to the PL spectrum. The bias dependence of the EFR intensity is plotted in Fig. 8. Similarly, they are also consistent with the three-step feature appeared in the *C-V* profile [Fig. 3(b)]. In Fig. 8, the saturated E_1

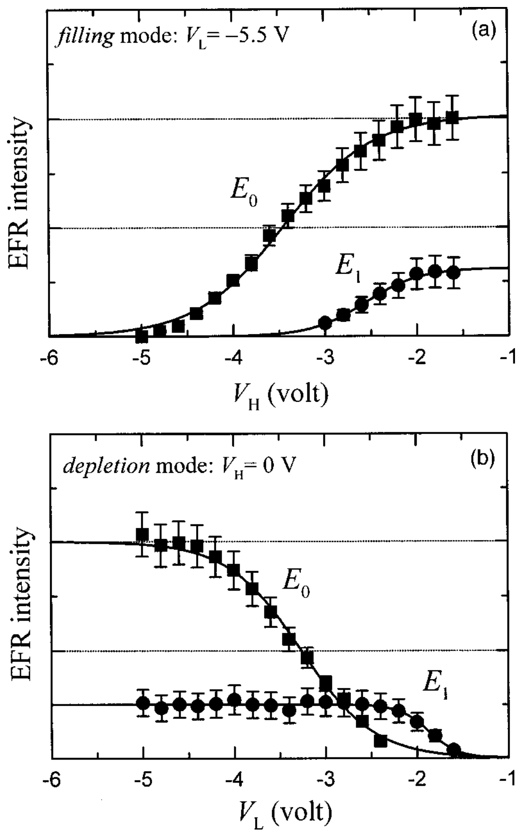

FIG. 6. Bias dependent EFR intensity for sample A in filling mode with $V_L = -5.5$ V (a) and depletion mode with $V_H = 0$ V. (b).

intensity is about two times larger than the E_0 intensity. Since the first excited QD state is fourfold degenerate, from these saturated intensities, we can estimate that the average electron occupancy may be ≈6–8 electrons per dot in sample B.

In our bias dependent EFR, an interesting state-filling feature was found. As seen in Fig. 7, the excited state transition always appeared before the ground-state transition was saturated. At low temperature limit, Fermi-Dirac distribution expects that energy level higher than the E_F cannot be occupied because the k_BT is very small. However, as shown in Fig. 8, the E_1 transition was still observable, even the filling bias was as low as −4.2 V. This state-filling feature is very similar to what was commonly observed in power dependent PL spectra.[16,17,25] But, it is important to mention that the origins for this feature appeared in both EFR and PL spectra are quite different. In PL spectra, luminescence intensities reflect a dynamical distribution of electron-hole pairs in the QD levels, which was resulting from several dynamic processes. At low temperatures, due to the lack of interdot charge transfers, carriers in a dot may not be in equilibrium with those in other dots.[16] Since the capture and recombination processes in a QD ensemble are random in nature,[16] the excited states would be populated before the ground states were fully occupied.

However, in contrast to the PL, the EFR measured a quasistatic distribution for the electrons in the QD's. As the electrons are injected by the filling bias, the system would establish an equilibrium charge transfer between the QD's and the barrier, because the time interval of the filling bias is long compared to the carrier transfer time. In other words,

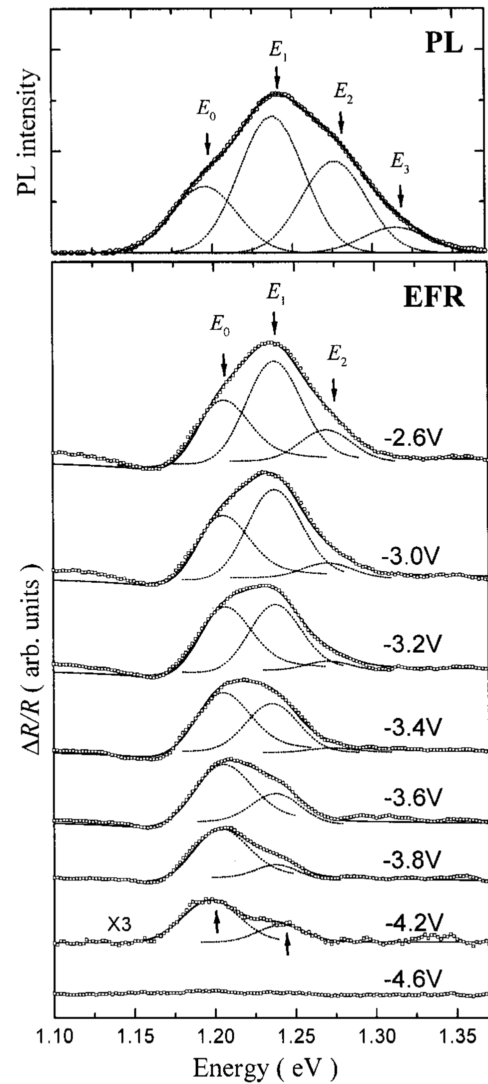

FIG. 7. The upper panel is the PL spectrum measured at $T = 10$ K and the lower panel shows the bias dependent EFR spectra for sample B with $V_L = -5.0$ V and varied V_H. The dotted lines are fitting lineshapes.

electrons in a dot should also be in equilibrium with those in other dots. However, the EFR intensities suggest that the excited states are still populated before the ground state is fully occupied. We explain this effect to an *inhomogeneous*

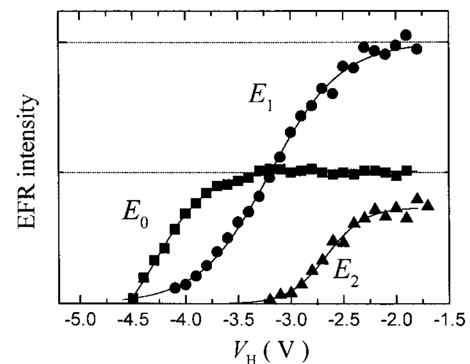

FIG. 8. The EFR intensities for each QD state appearing in Fig. 7.

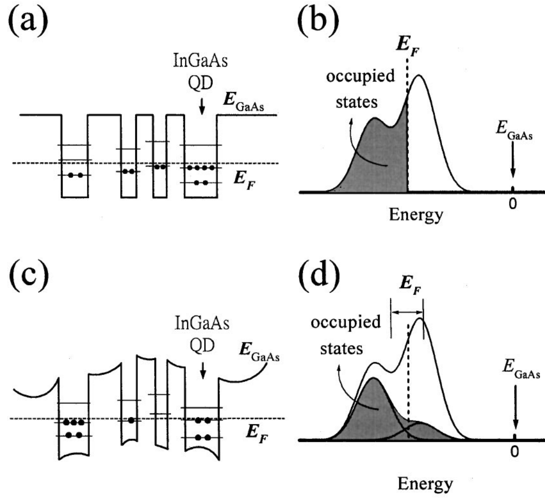

FIG. 9. Schematic diagrams for the electron level occupation in an *uncorrelated* QD system (a) and the corresponding occupied states (shadow area) (b). Schematic diagrams for the electron level occupation in a *correlated* QD system (c) and the corresponding occupied states (d).

distribution near the E_F, due to the correlated charge transfer among the QD's and the n-type environment. As is schematically depicted in Fig. 9(a), due to the size fluctuation, the confined energies of QD states were dispersed. If the charging of different QD's are *uncorrelated*, the QD levels with energy below the E_F will be completely filled. In this case, the GaAs conduction band edge (E_{GaAs}) can be taken as an energy reference for the QD density of state (DOS). Thus the occupied states show a truncated behavior at E_F, which is depicted schematically as the shadow region in Fig. 9(b). However, the confined energy and the n-doped environment determine the electron filling in a QD. Different QD's with different confinement energies would induce different band bending around the QD's. Moreover, since the interdot distance is randomly distributed, the depletion regions for some

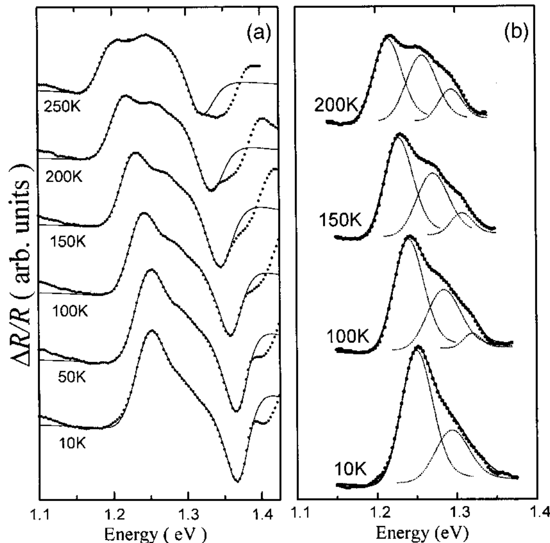

FIG. 10. (a) Experimental EFR spectra (●) and fitting lineshapes (solid lines) at various temperatures. (b) The EFR spectra (●) and fitting lineshapes (solid and dotted lines) after subtracting the fitted WL signal.

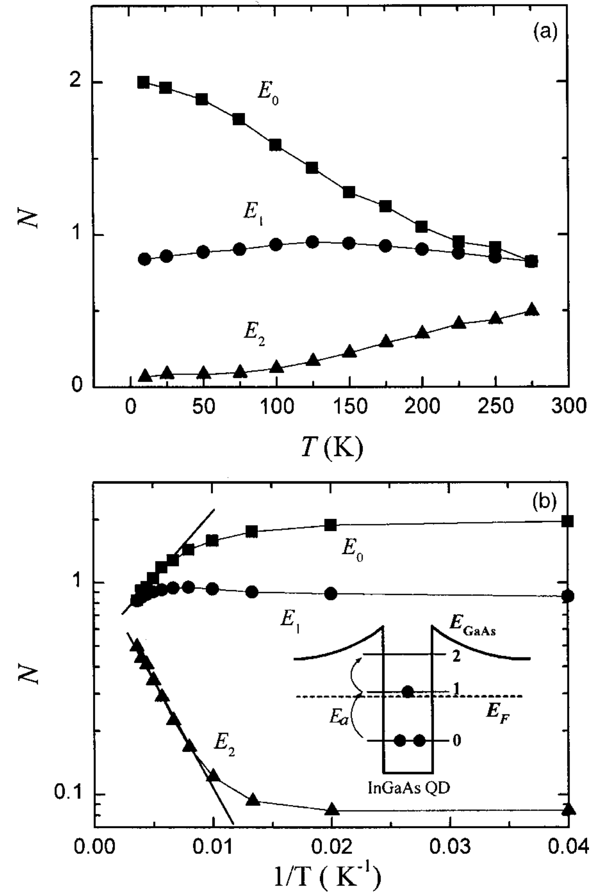

FIG. 11. (a) Temperature dependence of the QD level occupation deduced from the EFR intensity. (b) Arrhenius plot to the QD level occupation.

closely packed QD's may mutually overlap. Therefore, the electron level filling in different QD's are strongly *correlated* by the n-type environment. This effect is schematically depicted in Fig. 9(c). In this situation, the relative E_F positions in different dots, with respect to the GaAs band edge, are no longer the same. If we still plot the QD DOS with respect to the E_{GaAs}, as shown in Fig. 9(d), the E_F will be dispersed into a ''band'' and the truncated behavior of occupied states will disappear. This explains why we observed the appearance of E_1 transition before the ground states were fully occupied.

C. Thermal distributions

We have investigated the temperature evolution of the EFR spectra. Figure 10(a) shows the EFR spectra for sample A measured at various temperatures, with $V_{\mathrm{L}}=-5.5\,\mathrm{V}$ and $V_{\mathrm{H}}=0\,\mathrm{V}$. The fitting lineshapes, considering the intensity-modulation Gaussian lineshapes, are also shown for comparison. In order to see the QD signals more clearly, we subtracted the WL signal from these spectra, which are shown in Fig. 10(b). In this figure, an increase in temperature modifies the relative intensities of the QD transitions. With the increasing temperature, the E_0 intensity is decreased, while the excited states are increased. These EFR intensities can be correlated to the electron thermal distribution in the QD's. If we assume that the ground states are fully occupied

at $T = 10$ K, i.e., $N = 2$, the level occupations at different temperatures can be deduced from the relative EFR intensities. In Fig. 11(a), we show the temperature dependence of the level occupation for each QD state, and the corresponding Arrhenius plot is shown in Fig. 11(b). As discussed above, sample A contains ≈ 2–3 electrons per dot at $T = 10$ K. Therefore, the Fermi level E_F may be lying just below the first excited state (see the inset). With the increasing temperature, the electrons in the ground state were thermally populated to the first excited state. By a linear fit to the decreasing part of the E_0 occupancy, we extract an activation energy of $E_{a,0\rightarrow 1} = 27(\pm 5)$ meV, for the electrons in QD ground state. Because the electrons in the first excited state can also be thermally occupied to the second excited state, the E_1 occupancy did not change significantly. At low temperatures, the second excited states are empty, implying that the increasing electrons are coming from the first excited state. By using the increasing part of the E_2 occupancy, we obtained an activation energy of $E_{a,1\rightarrow 2} = 34(\pm 5)$ meV, for the electrons thermally populated to the second excited state. In *C-V* measurements, we found that the electron interlevel splitting is ≈ 78 meV, including the effect of Coulomb charging energy. Interestingly, the obtained activation energies of $E_{a,0\rightarrow 1} = 27(\pm 5)$ is quite close to the electron interlevel spacing of ≈ 30 meV in neutral dots, i.e., without Coulomb charging energy. Because these electrons are already in the QD's, thermal population to a higher state do not require Coulomb charging energy.

IV. CONCLUSION

In summary, we have performed the PL, *C-V* and EFR measurements to investigate the $In_{0.5}Ga_{0.5}As$ self-assembled QD ensemble. The electronic structures of the QD's were constructed by *C-V* profile. Coulomb charging effects on the electronic structures were found to be non-negligible. The electron level occupations were measured by the EFR spectra. Due to the correlated carrier transfer among the QD's and the *n*-type environment, the electron level filling is inhomogeneous near the E_F. Finally, the thermal population in the QD levels was investigated. The activation energies for the thermal population were found to be close to the level splitting, which means that electrons thermally populated to higher state do not require Coulomb charging energy.

ACKNOWLEDGMENTS

The authors would like to thank the Optical Center of the National Central University for the use of its MBE system. This work was supported in part by the National Science Council of the Republic of China under Grant No. NSC 88-2112-M-008-003.

APPENDIX: INTENSITY-MODULATION LINESHAPE MODEL

For the jth QD interband transition, the dielectric function $\tilde{\varepsilon}$ is given by

$$\tilde{\varepsilon}(A_j, E-E_j) = \varepsilon_R + i\varepsilon_I = 1 + A_j(L_R + iL_I), \tag{A1}$$

where ε_I and ε_R are the imaginary and real parts of the dielectric function, A_j and E_j are the intensity and energy of the jth transition, L_I and L_R are the lineshape functions related to the imaginary and real parts of the dielectric function. Due to the QD size fluctuations, the L_I can be assumed to be a Gaussian function and L_R can be obtained by a Kramer-Kroning relation,[27]

$$L_I(E-E_j, \Gamma) = -\frac{1}{\Gamma\sqrt{\pi/2}} \exp[-2(E-E_j)^2/\Gamma^2], \tag{A2}$$

$$L_R(E-E_j, \Gamma) = \frac{(E-E_j)}{\Gamma^2} H(1;3/2;-2(E-E_j)^2/\Gamma^2), \tag{A3}$$

where $H(a;b;z)$ is the confluent hypergeometric function. Taking into account the Pauli-blocking effect, the A_j also dependent on the electron occupation N_j, which can be expressed as

$$A_j(N_j) = g_j - N_j. \tag{A4}$$

If the charging states are modulated between being empty and completely filled, the change in the dielectric function $\Delta\tilde{\varepsilon}$ is given by

$$\begin{aligned}\Delta\tilde{\varepsilon} &= \tilde{\varepsilon}(g_j, E-E_j) - \tilde{\varepsilon}(g_j - n_j, E-E_j) \\ &\approx N_j[L_R(E-E_j, \Gamma) + iL_I(E-E_j, \Gamma_j)],\end{aligned} \tag{A5}$$

which is directly proportional to the corresponding occupation N_j and is essentially a intensity-modulation lineshape. Finally, the spectrum, $\Delta R/R$, can be expressed as

$$\Delta R/R \sim \sum_{j=0}^{2} N_j e^{i\theta}(\alpha - i\beta)[L_R(E-E_j, \Gamma) + iL_I(E-E_j, \Gamma)], \tag{A6}$$

where C_j is a normalization constant, θ is a phase factor, α and β are the Seraphine coefficients.

[1] D. Bimberg, M. Grundmann, and N. N. Ledentsov, *Quantum Dot Heterostructures* (Wiley, Chichester, 1999).

[2] M. Sugawara, *Self-assembled InGaAs/GaAs Quantum Dots*, Vol. 60 of Semiconductor and Semimetals, edited by R. K. Willardson and E. R. Weber (Academic Press, New York, 1999).

[3] N. Kirstaedter, O. G. Schmidt, N. N. Ledentsov, D. Bimberg, V. M. Ustinov, A. Yu. Egorov, A. E. Zhukov, M. V. Maximov, P. S. Kop'ev, and Zh. I. Alferov, Appl. Phys. Lett. **69**, 1226 (1996).

[4] M. V. Maximov, Yu. M. Shernyakov, A. F. Tsatsul'nikov, A. V. Lunev, A. V. Sakharov, V. M. Ustinov, A. Yu. Egorov, A. E. Zhukov, A. R. Kovsh, P. S. Kop'ev, L. V. Asryan, Zh. I. Alferov, N. N. Ledentsov, D. Bimberg, A. O. Kosogov, and P. Werner, J. Appl. Phys. **83**, 5561 (1998).

[5] J. J. Finley, M. Skalitz, M. Arzberger, A. Zrenner, G. Böhm, and G. Abstreiter, Appl. Phys. Lett. **73**, 2618 (1998).

[6] M. C. Bödefeld, R. J. Warburton, K. Karrai, J. P. Kotthaus, G. Medeiros-Ribeiro, and P. M. Petroff, Appl. Phys. Lett. **74**, 1839 (1999).

[7] T. Lundstrom, W. Schoenfeld, H. Lee, and P. M. Petroff, Science **286**, 2312 (1999); W. V. Schoenfeld, T. Lundstrom, P. M. Petroff, and D. Gershoni, Appl. Phys. Lett. **74**, 2194 (1999).

[8] S. Raymond, S. Fafard, P. J. Poole, A. Wojs, P. Hawrylak, S. Charbonneau, D. Leonard, R. Leon, P. M. Petroff, and J. L. Merz, Phys. Rev. B **54**, 11 548 (1996).

[9] M. J. Steer, D. J. Mowbray, W. R. Tribe, M. S. Skolnick, M. D. Sturge, M. Hopkinson, A. G. Cullis, C. R. Whitehouse, and R. Murray, Phys. Rev. B **54**, 17 738 (1996).

[10] H. Drexler, D. Leonard, W. Hansen, J. P. Kotthaus, and P. M. Petroff, Phys. Rev. Lett. **73**, 2252 (1994).

[11] G. Medeiros-Ribeiro, F. G. Pikus, P. M. Petroff, and A. L. Efros, Phys. Rev. B **55**, 1568 (1997).

[12] B. T. Miller, W. Hansen, S. Manus, R. J. Luyken, A. Lorke, J. P. Kotthaus, S. Huant, G. Medeiros-Ribeiro, and P. M. Petroff, Phys. Rev. B **56**, 6764 (1997).

[13] R. J. Warburton, C. S. Dürr, K. Karrai, J. P. Kotthaus, G. Medeiros-Ribeiro, and P. M. Petroff, Phys. Rev. Lett. **79**, 5282 (1997).

[14] K. H. Schmidt, G. Medeiros-Ribeiro, and P. M. Petroff, Phys. Rev. B **58**, 3597 (1998).

[15] R. J. Warburton, B. T. Miller, C. S. Dürr, C. Bödefeld, K. Karrai, J. P. Kotthaus, G. Medeiros-Ribeiro, P. M. Petroff, and S. Huant, Phys. Rev. B **58**, 16 221 (1998).

[16] M. Grundmann and D. Bimberg, Phys. Rev. B **55**, 9740 (1997).

[17] K. Mukai, N. Ohtsuka, H. Shoji, and M. Sugawara, Appl. Phys. Lett. **68**, 3013 (1996).

[18] H. Jiang and J. Singh, J. Appl. Phys. **85**, 7438 (1999).

[19] G. Medeiros-Ribeiro, D. Leonard, and P. M. Petroff, Appl. Phys. Lett. **66**, 1767 (1995).

[20] S. Anand, N. Carlsson, M. E. Pistol, L. Samuelson, and W. Seifert, Appl. Phys. Lett. **67**, 3016 (1995).

[21] P. N. Brounkov, A. Polimeni, S. T. Stoddart, M. Henini, L. Eaves, P. C. Main, A. R. Kovsh, Yu. G. Musikhin, and S. G. Konnikov, Appl. Phys. Lett. **73**, 1092 (1998).

[22] T. M. Hsu, W.-H. Chang, K. F. Tsai, J.-I. Chyi, N. T. Yeh, and T. E. Nee, Phys. Rev. B **60**, R2189 (1999).

[23] C. M. A. Kapteyn, F. Heinrichsdorff, O. Stier, R. Heitz, M. Grundmann, N. D. Zakharov, D. Bimberg, and P. Werner, Phys. Rev. B **60**, 14 265 (1999).

[24] S. Raymond, X. Guo, J. L. Merz, and S. Fafard, Phys. Rev. B **59**, 7624 (1999).

[25] R. Leon, S. Marcinkevius, X. Z. Liao, J. Zou, D. J. H. Cock-ayne, and S. Fafard, Phys. Rev. B **60**, R8517 (1999).

[26] K. H. Schmidt, G. Medeiros-Ribeiro, M. Oestreich, P. M. Petroff, and G. H. Döhler, Phys. Rev. B **54**, 11 346 (1996).

[27] F. H. Pollak, *Handbook on Semiconductor*, edited by M. Balkanski (North Holland, New York, 1994), Vol. 2.